Frequency Identification of a Memory Polynomial Model for PA Modeling

Stanislas Dubois, Bruno Lelong, Jean-Michel Hode, Guillaume Ferre, Dominique Dallet

▶ **To cite this version:**

Stanislas Dubois, Bruno Lelong, Jean-Michel Hode, Guillaume Ferre, Dominique Dallet. Frequency Identification of a Memory Polynomial Model for PA Modeling. 2022 IEEE International Instrumentation and Measurement Technology Conference (I2MTC), May 2022, Ottawa, Canada. pp.1-6, 10.1109/I2MTC48687.2022.9806582 . hal-04297207

HAL Id: hal-04297207
https://hal.science/hal-04297207

Submitted on 21 Nov 2023

HAL is a multi-disciplinary open access archive for the deposit and dissemination of scientific research documents, whether they are published or not. The documents may come from teaching and research institutions in France or abroad, or from public or private research centers.

L'archive ouverte pluridisciplinaire **HAL**, est destinée au dépôt et à la diffusion de documents scientifiques de niveau recherche, publiés ou non, émanant des établissements d'enseignement et de recherche français ou étrangers, des laboratoires publics ou privés.

This full text paper was peer-reviewed at the direction of IEEE Instrumentation and Measurement Society prior to the acceptance and publication.

Frequency Identification of a Memory Polynomial Model for PA Modeling

Stanislas Dubois[1,2], Bruno Lelong[2], Jean-Michel Hodé[2], Guillaume Ferré[1], Dominique Dallet[1]
Univ. Bordeaux, Bordeaux INP, CNRS, IMS, UMR 5218, Talence (FRANCE)[1]
Thales DMS, Elancourt (FRANCE)[2]
Email: forename.name@{ims-bordeaux.fr[1], fr.thalesgroup.com[2]}

2022 IEEE International Instrumentation and Measurement Technology Conference (I2MTC) | 978-1-6654-8360-5/22/$31.00 ©2022 IEEE | DOI: 10.1109/I2MTC48687.2022.9806582

***Abstract*—In this paper, we describe the validation of the modeling of a power amplifier. The model used is a memory polynomial model. We propose a method of identification in the frequency domain, from characteristic points (in amplitude and in phase) which are the fundamental and the inter-modulation tones. We then describe the realization of a test-bench suitable for the validation of this model.**

***Index Terms*—Power Amplifier, Characterization, Modeling, Test-bench**

I. Introduction

The PA is a component electronically limited by two phenomenons, non-linearity, and memory effect. These two phenomenons degrade the output signal. In the frequency domain, these distortions are characterized by spurious tones on the spectrum of the amplified signal. The objective of power amplifier behavioral modeling is to model the distortion induced by amplification, in order to correct it, to linearize the component. This correction can be performed for example by pre-distortion or post-distortion techniques [1]–[3].

The issues with behavioral modeling are therefore multiple. First of all, it is necessary to accurately reproduce the behavior of the PA. There is therefore a first criterion of accuracy. Secondly, there is a criterion of computational complexity, relying in the number of coefficients needed. In general, the more accurate a model is, the larger the number of coefficients it requires. Finally, with all behavioral models, the question of identifying the parameters arises.

In the literature, a certain number of works are based on the method of least squares (LS) [4] for the model inversion. Derived adaptive methods such as least mean squares (LMS) or recursive least squares (RLS) methods, can be found [5]. In this paper, we propose a method of identifying parameters based on the observation in the frequency domain of characteristic points of the signal at the input of the PA, the reference signal, and of the signal at the output of the PA, the distorted signal.

This identification method presents linear computational complexity with the number of parameters to be estimated. It is therefore interesting compared to traditional inversion methods based on least squares, quadratic computational according to the number of parameters. This method, on the other hand, is only suitable for a characterization or foreground calibration context, where the input signal is known and where the characteristic points of the spectrum allowing the identification of the model are therefore known.

This paper is structured around four parts. In the first one, the model used is developed as well as the proposed identification method. Subsequently, a test bench is carried out in order to validate the model. The following two parts thus deal with the means of measurement and the constraints associated with this test bench, then with the characterization and measurements carried out with the PA. The last part finally deals with the validation of the model.

II. Model

Several behavioral models exist, allowing the reproduction of non-linear behavior as well as memory effects. The most comprehensive one is the Volterra model [6], [7], and a significant part of the literature deals with the simplification of this model [8]. Mention may in particular be made of the models of Wiener, Hammerstein [9]–[11], Wiener-Hammerstein [3], memory polynomial [12], [13], or generalized memory polynomial [14]. Our approach is based on the memory polynomial model, for reasons of complexity and accuracy [8], but also because the structure of this model allows the design of the proposed identification method, as will be seen further.

A. Model presentation

This model, linking the analytical form of the entry signal z to the output signal s is given by,

$$s_n = \sum_{k=0}^{p} \sum_{m} h_m^{(k)} z_{n-m} \left| z_{n-m} \right|^{2k} \tag{1}$$

with p the order of the polynomial expression of the model, translating the order of non-linearities, and m the memory depth of the model. In our approach, we are only interested in close-carrier non-linearities, being the inter-modulation products. It implies that only odd orders of non-linearities, hence the $2k$ exponent on the squared module, appear in the expression.

$h^{(k)}$ can be interpreted as filter impulse responses, one for each degree of non-linearity. These filters are responsible for the modeling of memory effect. Indeed, in the presence of a sinusoidal signal, its temporal periodicity, and therefore its redundancy, makes it possible to consider that memory effect

Authorized licensed use limited to: THALES DMS FRANCE SAS (926). Downloaded on November 21,2023 at 09:20:09 UTC from IEEE Xplore. Restrictions apply.
978-1-6654-8360-5/22/$31.00 ©2022 IEEE

linking each sample to their past samples, is translated to the samples of its neighborhood.

The model was chosen first of all because of its ability to emphasize non-linearity and memory effects with low computational cost. Secondly and more importantly, it was chosen due its structure separated between non-linearity and memory effect. It indeed consists in the cascade of blocks, of polynomial non-linearity without memory effect, and then with linear filtering (cf. Fig. 1). This structure makes it possible to design this identification method.

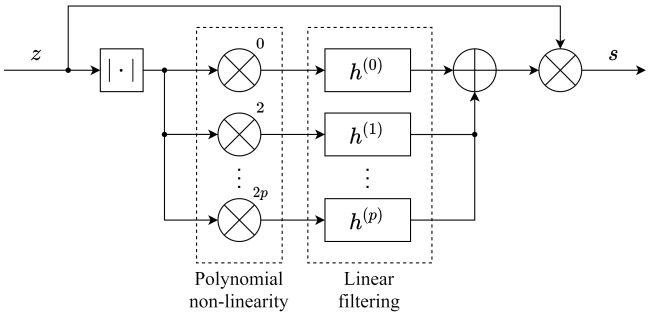

Fig. 1: Memory-polynomial model

In the frequency domain, equation (1) becomes,

$$s = z \sum_{k=0}^{p} H^{(k)} \left|z\right|^{2k} \tag{2}$$

with $H^{(k)}$ the frequency responses of our filters.

We will be interested here in the modeling of the gain of the power amplifier under test (frequency response $H^{(0)}$), as well as the inter-modulation products of orders 3, 5 and 7 (IMD3, IMD5 and IMD7). These correspond respectively to $H^{(1)}$, $H^{(2)}$ and $H^{(3)}$ frequency responses.

In this case the previous equation is then simplified to

$$s = z \sum_{k=0}^{3} H^{(k)} \left|z\right|^{2k} \tag{3}$$

B. Model development

The power amplifier (PA) modeling is therefore done by determining the frequency responses H. To do this, we needed to carry out a series of measurements at different frequencies and at different levels.

In order to bring-up the inter-modulation spurs, the identification will be performed on two-tone analytical signal z of the form,

$$z(t) = a_1 e^{j\omega_1 t} + a_2 e^{j\omega_2 t} \tag{4}$$

with ω_1 and ω_2 the pulsations of the two tones of respective frequencies f_1 and f_2 ($\omega_i = 2\pi f_i$), and a_1 and a_2 the complex coefficients reflecting the amplitude and the phase of the associated tones.

From equations (3) and (4), the model linking input $z(t)$ to output $s(t)$ is given by

$$\left\{\begin{array}{rl} z(t) = & ae^{j\phi_-}e^{j\omega_1 t} + ae^{j\phi_+}e^{j\omega_2 t} \\ s(t) = & H_{0-}e^{j\omega_1 t} + H_{0+}e^{j\omega_2 t} \\ + & H_{1-}e^{j(2\omega_1-\omega_2)t} + H_{1+}e^{j(2\omega_2-\omega_1)t} \\ + & H_{2-}e^{j(3\omega_1-2\omega_2)t} + H_{2+}e^{j(3\omega_2-2\omega_1)t} \\ + & H_{3-}e^{j(4\omega_1-3\omega_2)t} + H_{3+}e^{j(4\omega_2-3\omega_1)t} \end{array}\right. \tag{5}$$

with $a_1 = ae^{j\phi_-}$ and $a_2 = ae^{j\phi_+}$, assuming that both tones are emitted at the same level, and $H_{i\pm}$ expressed as follows:

$$\begin{aligned}
H_{0-} &= e^{j\phi_-}\left[H^{(0)}a + H^{(1)}3a^3 + H^{(2)}10a^5 + H^{(3)}35a^7\right] \\
H_{0+} &= e^{j\phi_+}\left[H^{(0)}a + H^{(1)}3a^3 + H^{(2)}10a^5 + H^{(3)}35a^7\right] \\
H_{1-} &= e^{j(2\phi_- - \phi_+)}\left[H^{(1)}a^3 + H^{(2)}5a^5 + H^{(3)}21a^7\right] \\
H_{1+} &= e^{j(2\phi_+ - \phi_-)}\left[H^{(1)}a^3 + H^{(2)}5a^5 + H^{(3)}21a^7\right] \\
H_{2-} &= e^{j(3\phi_- - 2\phi_+)}\left[H^{(2)}a^5 + H^{(3)}7a^7\right] \\
H_{2+} &= e^{j(3\phi_+ - 2\phi_-)}\left[H^{(2)}a^5 + H^{(3)}7a^7\right] \\
H_{3-} &= e^{j(4\phi_- - 3\phi_+)}H^{(3)}a^7 \\
H_{3+} &= e^{j(4\phi_+ - 3\phi_-)}H^{(3)}a^7
\end{aligned}$$

C. Model identification

In order to construct the frequency responses $H^{(0)}$, $H^{(1)}$, $H^{(2)}$, and $H^{(3)}$, of the filters modeling the amplifier, the coefficients a, ϕ_-, and ϕ_+ are deduced from the Fourier transform of the reference signal, and the coefficients $H_{k\pm}$, from the Fourier transform of the distorted signal. This means that two FFT have to be computed, one for the signal at the input of the PA, and one for the signal at its output.

The frequency responses of the filters of the model are then given by:

$$\begin{aligned}
a^7H^{(3)} &= \frac{1}{2}\left(H_{3-}e^{-j(4\phi_- - 3\phi_+)} + H_{3+}e^{-j(4\phi_+ - 3\phi_-)}\right) \\
a^5H^{(2)} &= \frac{1}{2}\left(H_{2-}e^{-j(3\phi_- - 2\phi_+)} + H_{2+}e^{-j(3\phi_+ - 2\phi_-)}\right) \\
&\quad - \frac{7}{2}\left(H_{3-}e^{-j(4\phi_- - 3\phi_+)} + H_{3+}e^{-j(4\phi_+ - 3\phi_-)}\right) \\
a^3H^{(1)} &= \frac{1}{2}\left(H_{1-}e^{-j(2\phi_- - \phi_+)} + H_{1+}e^{-j(2\phi_+ - \phi_-)}\right) \\
&\quad - \frac{5}{2}\left(H_{2-}e^{-j(3\phi_- - 2\phi_+)} + H_{2+}e^{-j(3\phi_+ - 2\phi_-)}\right) \\
&\quad + \frac{14}{2}\left(H_{3-}e^{-j(4\phi_- - 3\phi_+)} + H_{3+}e^{-j(4\phi_+ - 3\phi_-)}\right) \\
a^7H^{(0)} &= \frac{1}{2}\left(H_{0-}e^{-j\phi_-} + H_{0+}e^{-j\phi_+}\right) \\
&\quad - \frac{3}{2}\left(H_{1-}e^{-j(2\phi_- - \phi_+)} + H_{1+}e^{-j(2\phi_+ - \phi_-)}\right) \\
&\quad + \frac{5}{2}\left(H_{2-}e^{-j(3\phi_- - 2\phi_+)} + H_{2+}e^{-j(3\phi_+ - 2\phi_-)}\right) \\
&\quad - \frac{7}{2}\left(H_{3-}e^{-j(4\phi_- - 3\phi_+)} + H_{3+}e^{-j(4\phi_+ - 3\phi_-)}\right)
\end{aligned}$$

In time domain, modeling filters impulse responses are finally obtained by IFFT of the frequency responses $H^{(0)}$,

Authorized licensed use limited to: THALES DMS FRANCE SAS (926). Downloaded on November 21,2023 at 09:20:09 UTC from IEEE Xplore. Restrictions apply.

$H^{(1)}$, $H^{(2)}$ and $H^{(3)}$. These filters $h^{(k)}, k \in [\![0;3]\!]$, allow in the end to reproduce the behaviour of the amplifier.

III. Test setup

To validate the model presented previously, a test- bench allowing the simultaneous capture of the signal at the input of the PA, and the signal at its output, is needed, in order to be able to compare them. These signals will be referred to in the following, as respectively the reference signal, and the distorted signal.

A. Test-bench synoptic

The synoptic diagram of the measuring bench can be observed in Fig. 2.

The studied PA is in practice made up of several cascade amplifiers. This chain of amplifiers is designed to operate in compression phase, where it presents the best performance. The different levels of attenuation in the assembly were therefore studied so as to keep the chain in compression, based on the input powers. These attenuation levels were also chosen so that the signals arrived with similar powers at the input of the oscilloscope, in its optimum level range with respect to its linearity performance (inter-modulation).

A photo of the test-bench thus produced is shown in Fig. 3. On this picture can be seen at the top left the PA under study (gray box), above the oscilloscope. On the right two VSGs from which the two-tones signal were initially generated, can be observed. Only one of these devices was used in practice.

The Vector Signal Generator (VSG) used here was a Rohde & Schwarz SMBV100-A, and the oscilloscope was a Keysight UXR. It allowed sampling at 4 GHz on 2 channels simultaneously.

B. Signal generation

The two tones used for the evaluation of the amplifier are generated by a single VSG. A file containing 4 points, $[1, 0, -1, 0]$, is used to describe a real cosine. This waveform is generated by the device in baseband. By setting the sampling frequency of this file, the inter-carrier can be controlled. This is the spacing between the two tones characteristics of a real cosine in the frequency domain. Let f_s be the sampling frequency of a baseband cosine, this waveform being defined on 4 points, this signal $s(t)$ is of the form:

$$s(t) = \cos\left(2\pi \frac{f_s}{4} t\right) \tag{6}$$

In the frequency domain, the spectrum of this real cosine will present two tones at $\frac{f_s}{4}$ and $\frac{f_s}{4}$. Spacing between these two tones, the inter-carrier of the two-tones signal, is $\frac{f_s}{2}$. The frequency sampling was therefore set to be twice the desired inter-carrier. This cosine was then modulated and put on carrier, the center frequency of the two-tone signal. All these operations were performed on the VSG, controlled from MATLAB, on the PC.

C. Reduction of measurement noise

It appeared important through measurement phase, to limit the measurement noise on the identification of inter-modulation products. The model indeed requires a measurement of the amplitudes of inter-modulation tones order up to 7. At low input levels, these peaks are quickly hidden by noise floor, unless the resolution of the Fourier transform is increased. This can be done by analysing longer acquisitions with more points, or by limiting the measurement noise by averaging each measure over a number of coherent acquisitions. In both cases, this means capturing samples on a longer period of time. However in the second case, this does not affect processing time on the PC.

Generating the signal from a file describing the baseband waveform on the VSG, allowed the addition of markers to the waveform file. These markers formed a second signal, sent to the oscilloscope, making it possible to trigger acquisitions on it. This process allowed, as long as the acquisitions made were coherent, to average them, in order to reduce the measurement noise, and therefore to improve the accuracy of the modeling.

IV. Power amplifier characterization

The test bench presented above allowed us to carry out a certain number of measurements, in order to characterize the PA under test in gain, and in linearity. Each factor was studied on varying input powers, in a frequency band ranging from a few MHz to 500 MHz.

A. Measurements

Here are in Fig. 4 an acquisition made in compression phase, with the presented test-bench. Time and frequency domain are plotted for the reference signal on top, and the distorted signal on the bottom.

The frequency resolution is chosen to be equal to the inter-carrier, to be as small as possible. This constrains time domain acquisitions to two periods of the inter-carrier frequency. Finally, the number of averages made to limit measurement-noise is determined according to a measurement time of 5 ms, constant across all measurements made, in order to maintain a constant SNR on the whole study.

The compression effect of the power amplifier can clearly be seen here, in time domain and in frequency domain. In time domain, it tends to flatten the waveform at extreme amplitudes. This results in spurious tones amplitudes increasing. A slight phase shift between the reference and distorted curves can also be observed. Indeed, although the acquisitions are simultaneously performed, there is a delay of the order of a few nanoseconds between the two channels, corresponding to the signal travel time in the coaxial cables and in the PA. This delay being constant throughout the whole manipulation, it will be estimated and corrected in MATLAB while processing.

B. Relative gain and inter-modulation

In Fig. 5a, the relative gain between reference and distorted signals, measured on the frequency band of interest, can be observed.

Authorized licensed use limited to: THALES DMS FRANCE SAS (926). Downloaded on November 21,2023 at 09:20:09 UTC from IEEE Xplore. Restrictions apply.

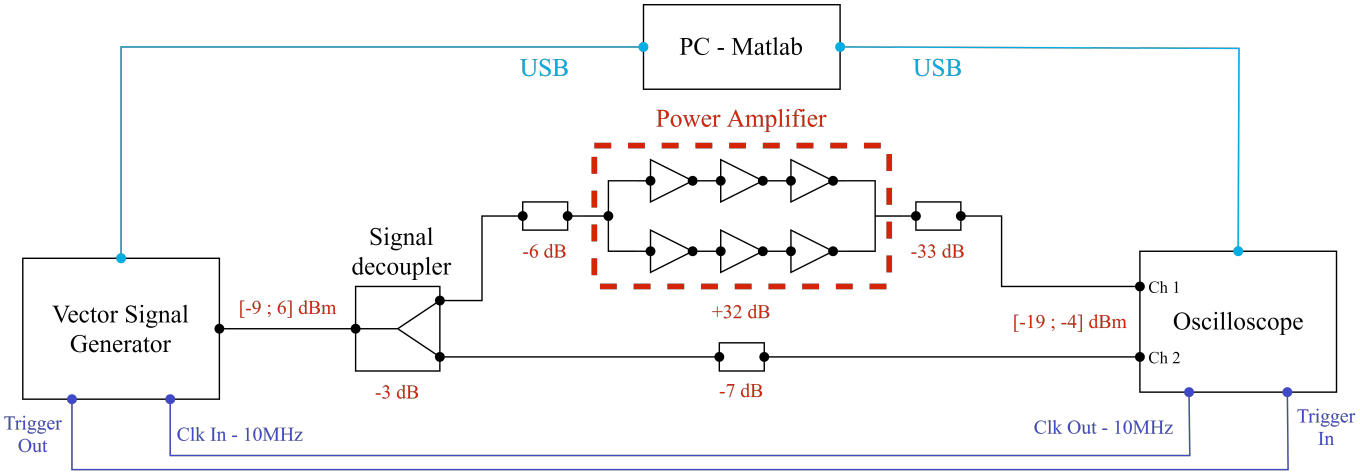

Fig. 2: Synoptic diagram of the measuring bench

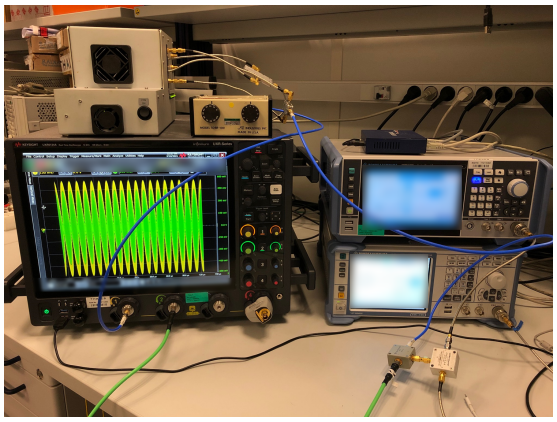

Fig. 3: Photo of the measuring bench

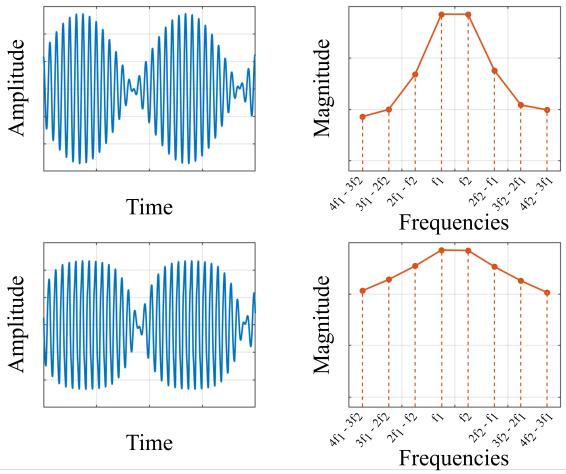

Fig. 4: Acquisition performed with the presented test-bench - Carrier: 100 MHz - Inter-carrier: 5 MHz

Two interesting things can be noticed. The first one is related to the variation of gain depending on the input power. The gain is indeed not constant and decreases as the level increases. This is the phenomenon of compression. Secondly, gain depends largely on the frequency of the signal, which justifies the choice of a model highlighting memory effects.

The evolution of inter-modulation products as a function of level and frequency, across the entire study band, are presented in Figs. 5b, 5c and 5d.

Inter-modulation products of orders 3, 5 and 7 have high amplitudes (up to -20 dBc of IMD3 at high entry levels). This is due among other things to compression and saturation, strongly non-linear phenomenons, which appear at higher input powers. In addition, these inter-modulation products evolve here once again, with the input power, but also with the frequency.

V. Model validation

From the measurements performed using the presented test-bench, the frequency responses of the model describing the behaviour of our amplifier, were computed.

A. Filters obtained

These filters, reflecting the amplitudes of the gain and of the inter-modulation products of orders 3, 5 and 7, are presented in Fig. 6. For each response, different curves are plotted for different inter-carrier values.

It can be observed first that this model is relatively robust to the variation of the inter-carrier. In addition, a large increase in the amplitude of the coefficients can be noticed, as the order of the signal increases. This is due to the fact that, the higher the order the signal is raised to, the more its values decrease, the initial signal being between -1 and 1.

B. Model validation

In Fig. 7 the result of the modeling of the relative gain as a function of the level, on all of the band of frequencies considered is presented. The result of the modeling of order 3 inter-modulation as a function of the level, on all the frequency band considered, can also be seen.

Authorized licensed use limited to: THALES DMS FRANCE SAS (926). Downloaded on November 21,2023 at 09:20:09 UTC from IEEE Xplore. Restrictions apply.

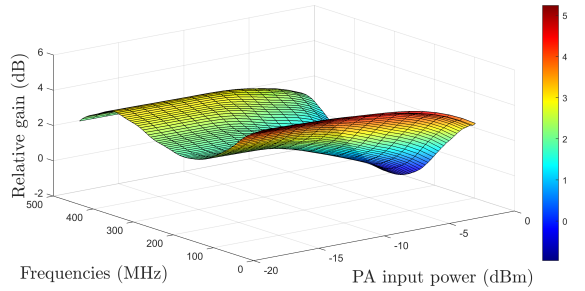

(a) Relative gain

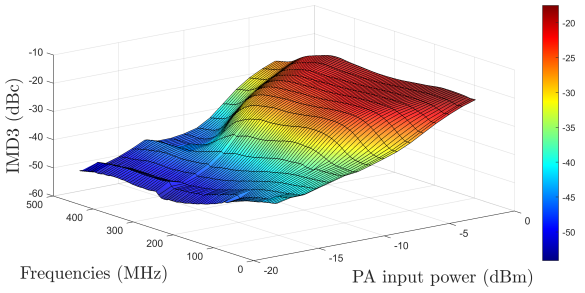

(b) Order 3 inter-modulation

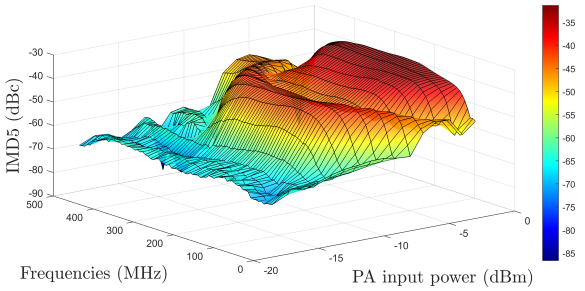

(c) Order 5 inter-modulation

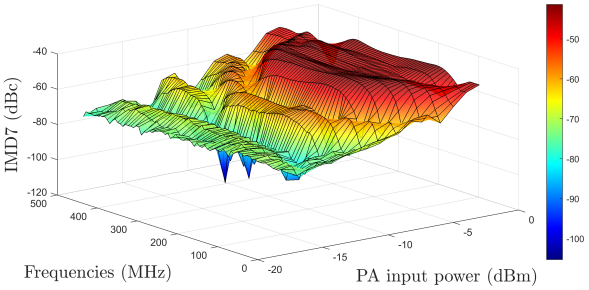

(d) Order 7 inter-modulation

Fig. 5: Evolution of measured relative gain and IMD3-5-7, across level and frequency

The gain modeling exactly reproduces the behavior observed in Fig. 5a, and the IMD3 modeling, although relatively inaccurate, follows the measurement trend (Fig. 5b).

This can be explained looking at the system of equations in section II-C. Indeed, the gain modeling is not only linear with the input power, but is also polynomial with the contributions

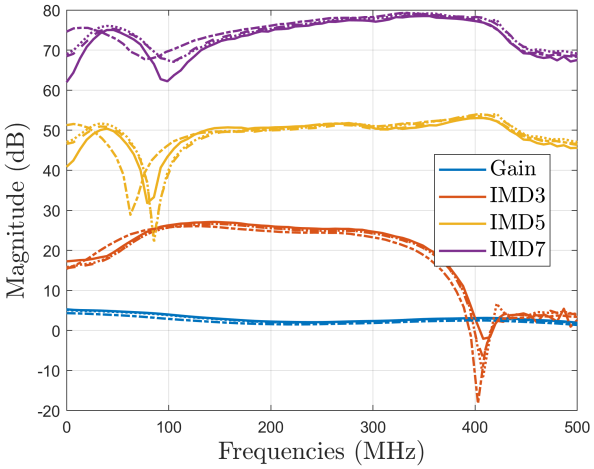

Fig. 6: Frequency responses of the model

of higher orders of non-linearities. Actually, the lower the order of the response is (order 0 corresponding to the gain), the more its modeling is faithful to the measurement.

This is why the modeling of non-linearities of orders 5 and 7 are not shown here. Their result is indeed very inaccurate, since the only utility of these measurements is to contribute to the accuracy of the modeling of lower orders responses.

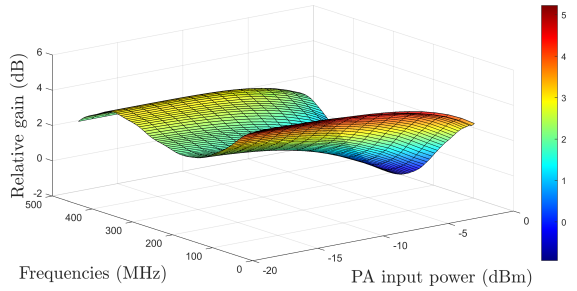

(a) Relative gain

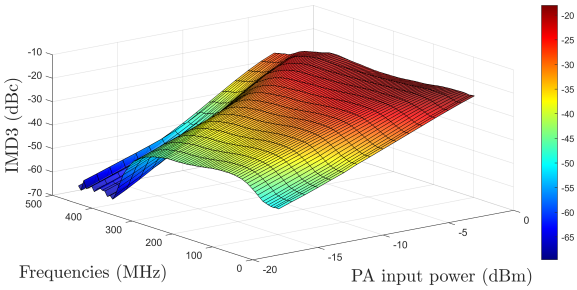

(b) Order 3 inter-modulation

Fig. 7: Evolution of modeled relative gain and IMD3, across level and frequency

To conclude quantitatively on the accuracy on the modeling, the relative deviations between the measures of gain and

Authorized licensed use limited to: THALES DMS FRANCE SAS (926). Downloaded on November 21,2023 at 09:20:09 UTC from IEEE Xplore. Restrictions apply.

IMD3, and their modeled versions, is presented in Fig. 8. Since these frequency responses were computed for several input powers, for each frequency, standard deviation is the result of the averaging of all relative deviations between the measurements, and their corresponding modeling.

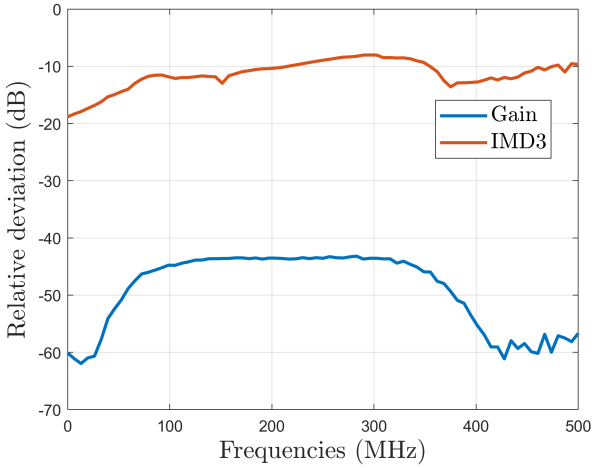

Fig. 8: Relative deviation between measured and modeled gain and distortion, averaged on every input power

The accuracy of the modeling on the gain seems largely sufficient here (under -40 dB of relative deviation between observed and modeled gain) in a context of characterization. The proposed identification method therefore allows the accurate estimation of the model parameters. The accuracy of the modeling however deteriorates with the IMD3. The objective of this model being to reproduce the amplification behavior (gain) of the PA under test, the model is validated. The inter-modulation products are once again only there to improve the precision of the computation of the filter modeling the gain, allowing its frequency response to be polynomial.

VI. Conclusion

In this paper, we proposed an identification method in the frequency domain, suitable for behavioral modeling of a PA, by a memory polynomial model. A test-bench was then presented, that allowed the validation of this model.

The relative difference between the measured gain and its modeling is below -40 dB, over the entire study band.

The method of identifying the parameters of the model presented made it possible to construct the frequency response of the gain of the amplifier as being a polynomial contribution of its observation, as well as observations of the inter-modulation products raised to their respective orders. The gain modeling is therefore all the more precise as there are contributions from the measurement of the inter-modulation products, and therefore as the observed order of non-linearity increases. Observing higher-order non-linearities would also allow the component's low-order non-linearities to be accurately modeled.

In-Fine, the limit here relies within computational complexity (the higher the order of non-linearity is, the more characteristic points there are to evaluate), but above all this limit is reached at the noise floor level. For components that have high performance in terms of linearity, it indeed becomes quite difficult (very long acquisitions) to observe with accuracy high-order inter-modulation products.

References

[1] J. K. Cavers, "Amplifier linearization using a digital predistorter with fast adaptation and low memory requirements," *IEEE Transactions on Vehicular Technology*, vol. 39, no. 4, pp. 374–382, 1990.

[2] K. Gumber and M. Rawat, "Low-cost rfin–rfout predistorter linearizer for high-power amplifiers and ultra-wideband signals," *IEEE Transactions on Instrumentation and Measurement*, vol. 60, no. 9, pp. 2069–2081, 2018.

[3] R. Vansebrouck, "Digital post-distortion for wideband receivers," Ph.D. dissertation, Telecom Paris Tech, 2016.

[4] S. Haykin, *Adaptative filter theory*, 2013.

[5] P. S. R. Diniz, *Adaptive Filtering: Algorithms and Practical Implementation*, 2008.

[6] M. Schetzen, *Nonlinear System Modelling and Analysis from the Volterra and Wiener Perspective*, 2010.

[7] S. Benedetto, E. Biglieri, and R. Daffara, "Modeling and performance evaluation of nonlinear satellite links-a volterra series approach," *IEEE Transactions on Aerospace and Electronic Systems*, vol. 15, no. 4, pp. 494–507, 1979.

[8] J. Tao, "Behavioral modeling and fpga implementation of digital predistortion for rf and microwave power amplifiers," Ph.D. dissertation, Politecnico di Torino, 2016.

[9] O. Nelles, *Nonlinear System Identification*, 2001.

[10] M. Schetzen, *The Volterra and Wiener Theories of Nonlinear Systems*, 2006.

[11] D. Wisell, J. Jalden, and P. Handel, "Behavioral power amplifier modeling using the lasso," *2008 IEEE Instrumentation and Measurement Technology Conference*, 2008.

[12] L. Ding, G. T. Zhou, D. R. Morgan, Z. Ma, J. S. Kenney, J. Kim, and C. R. Giardina, "Memory polynomial predistorter based on the indirect learning architecture," *Global Telecommunications Conference, 2002. GLOBECOM '02. IEEE*, 2002.

[13] ——, "A robust digital baseband predistorter constructed using memory polynomials," *IEEE Transactions on Communications*, 2004.

[14] D. R. Morgan, Z. Ma, J. Kim, M. G. Zierdt, and J. Pastalan, "A generalized memory polynomial model for digital predistortion of rf power amplifiers," *IEEE Transactions on Signal Processing*, vol. 54, no. 10, pp. 3852–3860, 2006.

Authorized licensed use limited to: THALES DMS FRANCE SAS (926). Downloaded on November 21,2023 at 09:20:09 UTC from IEEE Xplore. Restrictions apply.